The International Journal of Advanced Manufacturing Technology (2019) 102:3791–3800
https://doi.org/10.1007/s00170-019-03475-x

ORIGINAL ARTICLE

A new method for determining the instantaneous uncut chip thickness in micro-milling

Xiang Zhang[1] · Xudong Pan[1] · Guanglin Wang[1]

Received: 4 September 2018 / Accepted: 18 February 2019 / Published online: 28 February 2019

Abstract

The calculation accuracy of instantaneous uncut chip thickness (IUCT) plays a very important role in the modeling of milling processes. Tool runout is an obstacle to the accurate calculation of IUCT in micro-milling. This paper focuses on the calculation of IUCT and proposes a new method for determining the IUCT in micro-milling. Firstly, the effects of tool runout and single-edge cutting on nominal uncut chip thickness were analyzed. Then, the calculation methods of nominal uncut chip thickness and actual uncut chip thickness in micro-milling were proposed respectively, which took into account the impact of tool runout, single-edge cutting, intermittent chip formation, and the minimum chip thickness. The pseudo-single-edge cutting which may occur in single-edge cutting was discussed. Finally, nominal uncut chip thickness and actual uncut chip thickness in micro-milling were analyzed respectively. The calculated results showed higher accuracy compared to conventional method.

Keywords Instantaneous uncut chip thickness · Tool runout · Single-edge cutting · Micro-milling

1 Introduction

Micro-milling is a direct and effective manufacturing method which has high rate of material removal for manufacturing micro-structures [1, 2]. Surface quality, cutting forces, process stability, and other machining process performance are needed to be accurately predicted to establish automation or optimization model of the machining processes [3]. A key issue in such predictions is to calculate the instantaneous uncut chip thickness (IUCT), which plays a very important role in the modeling of milling processes as it is closely related to the cutting forces, tool life, machining quality, and process stability. However, tool runout is an obstacle to accurately calculate the IUCT which is caused by manufacturing and assembling errors that result in the deviation between tool axis and spindle axis [4]. In micro-milling, tool runout will significantly affect IUCT in two aspects. Firstly, the IUCTs of different cutting edge are not equal at the same cut depth. In some situations, only one cutting edge removes material effectively, which is the so-called single-edge cutting. Secondly, the IUCTs of the same edge change with the axial depth of cut because tool runout angle changes along with the helix angle of the milling cutter. Moreover, the single- and multiple-edge cutting alternate occur at different cutting depths which will lead the real cutting edge to withstand greater cutting force resulting in easier to wear or breakage.

Martellotti established cutting edge trajectories model and proposed an approximate algorithm for IUCT [5]. Spiewak established an analytical modeling of cutting edge trajectories in milling processes which used uniform transformation technique and matrix formulation of the tool geometry. And then, he proposed an improved IUCT computing method [6, 7]. Montgomery et al. analyzed the chatter vibration waves which were left on the milled surface and proposed a dynamic milling model in which the IUCT was calculated from cutting edges motion [8, 9].

As tool diameter and feed per tooth decreasing sharply, the calculation method of IUCT in conventional milling cannot be used directly in micro-milling. Bao et al. calculated the IUCT which took into account tool runout and trajectories of the tool tips and established a cutting force model in micro-milling [10, 11]. Vogler et al. proposed a mechanistic cutting force model which was based on the slip-line model. In their model, the minimum chip thickness was considered in the calculation of the IUCT [12]. Rodríguez et al. simplified the milling cutter as a cantilever beam which deflected under cutting force.

✉ Xiang Zhang
zhangxiang1982@hit.edu.cn

[1] School of Mechatronics Engineering, Harbin Institute of Technology, Harbin 150001, China

Then, the deflection was introduced into the calculation of IUCT [13]. Jun et al. computed the IUCT and established a cutting force model which included the elastic recovery of workpiece and dynamic deflection of tool [14]. Li et al. also established a cutting force model. In their model, tool runout and the minimum chip thickness were introduced in the calculation of IUCT [15].

At present, many methods for calculation IUCT have been proposed, but there are still some shortcomings in the calculation for IUCT in micro-milling. This paper proposes a new method for determining IUCT in micro-milling which considering tool runout, minimum chip thickness, single-edge cutting, and other factors. The proposed method can be applied not only in micro-end milling, but also in micro-side milling.

2 Tool runout and single-edge cutting

Figure 1 shows tool runout where O_s, O_t, and R are rotation center of spindle and milling cutter and tool radius respectively. Tool runout length r is defined as the distance between points O_s and O_t; tool runout angle θ is defined as the anti-clockwise angle between the line connecting points O_s and O_t and y-axis positive direction in the tool tip plane. k_1 and k_2 represent the first and second cutting edges which are set to 0 and 1, respectively. When single-edge cutting occurs, only one cutting edge has the real IUCT. Furthermore, tool runout angle varies along the tool helix angle, which results in different IUCTS of the same cutting edge in different axial position.

In micro-side milling, axial depth of cut cannot be neglected. Taking into account the helix lag angle $\alpha(z)$, single-edge cutting criterion can be written as

$$\zeta = f_t - |2r\cos(\alpha(z) + \theta)| \tag{1}$$

where f_t is feed per tooth; $\alpha(z)$ is the helix lag angle at axial height of z, which could be calculated as

$$\alpha(z) = z\tan\beta / R \tag{2}$$

where z is axial height of the milling cutter and the origin position is at the tool tip ($z = 0$); β is helix angle of the cutter.

In micro-end milling, the effect of axial position of the milling cutter could be ignored, so single-edge cutting criterion could be simplified as

$$\zeta = f_t - |2r\cos\theta| \tag{3}$$

3 Instantaneous uncut chip thickness algorithm

3.1 Nominal uncut chip thickness

The IUCT in conventional milling can be approximated by the following Eq. (5):

$$h_n(\gamma) = f_t \sin\gamma \tag{4}$$

where γ is position angle of the cutting edge.

Due to the little feed per tooth, tool runout, and single-edge cutting significantly affect the calculation of IUCT in micro-milling, as shown in Fig. 2. In this paper, nominal uncut chip thickness (NUCT) refers to the theoretical uncut chip thickness, without considering intermittent chip formation and minimum chip thickness. The NUCTs in multiple-edge cutting are shown in Fig. 2 a, b. When the tool has no runout, the NUCTs of each cutting edges are equal; when the tool has runout, the NUCTs of each cutting edges are obvious different. When single-edge cutting occurs, as shown in Fig. 2 c, only one cutting edge has the real NUCTs. From Fig. 2, it can be seen that Eq. (4) does not take into account the impact of tool runout and single-edge cutting. Therefore, it is unfavorably to be used to precisely calculate the NUCT in micro-milling.

Figure 3 shows the cutting edge trajectories at the axial height of z which taking into account tool runout. Feed direction is along the X-axis to simplify the model.

In this proposed NUCT algorithm, it is necessary to ensure that the current tool center point O_0 (x_0, y_0), the point on the previous cutting edge trajectory P_{ex} (x_{ex}, y_{ex}), and the point on the current cutting edge trajectory $P_0(x, y)$ are collinear, which satisfy the following equation:

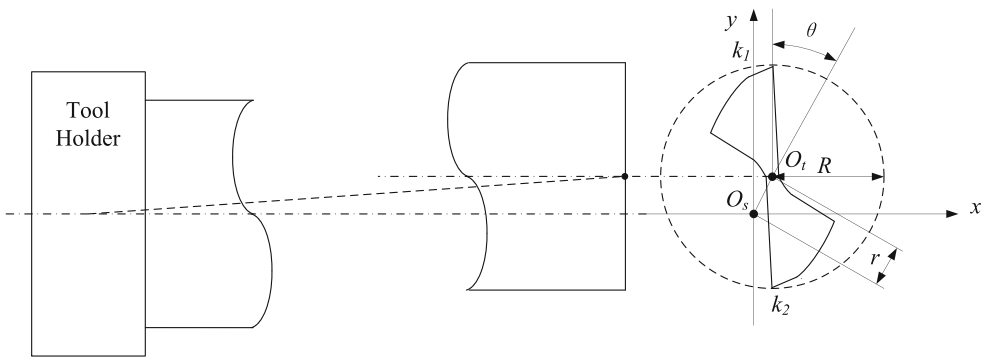

Fig. 1 Tool runout

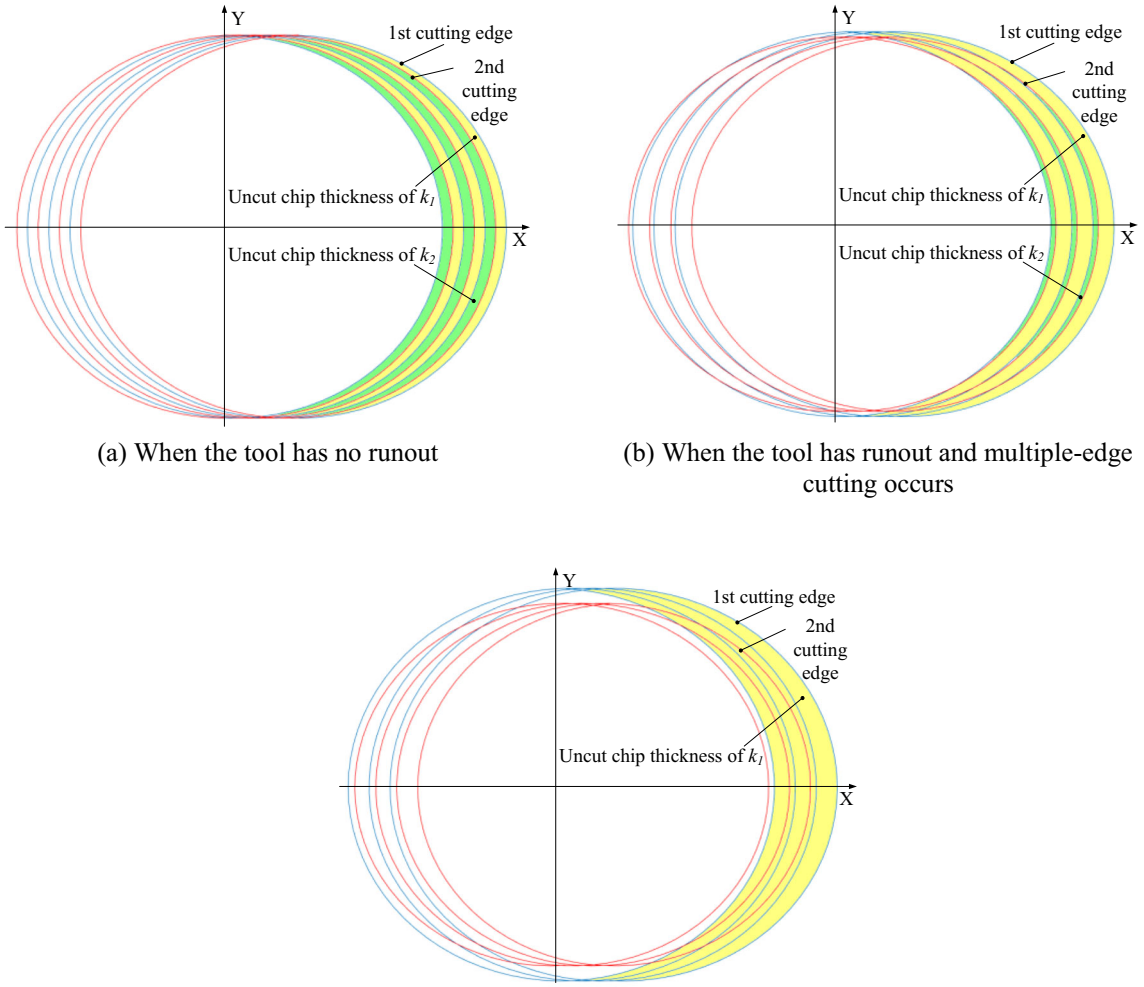

(a) When the tool has no runout

(b) When the tool has runout and multiple-edge cutting occurs

(c) When single-edge cutting occurs

Fig. 2 NUCTs in different situations. When the tool has no runout (**a**). When the tool has runout and multiple-edge cutting occurs (**b**). When single-edge cutting occurs (**c**)

$$(x_0-x)/(y_0-y) = (x-x_{ex})/(y-y_{ex}) \tag{5}$$

where

$$\begin{cases} x_0 = ft + r\sin(\omega t + \theta + \alpha(z)) \\ y_0 = r\cos(\omega t + \theta + \alpha(z)) \end{cases} \tag{6}$$

$$\begin{cases} x = ft + R\sin(\omega t - \pi k) + r\sin(\omega t + \theta + \alpha(z)) \\ y = R\cos(\omega t - \pi k) + r\cos(\omega t + \theta + \alpha(z)) \end{cases} \tag{7}$$

where f is feed rate, t is current cutting time, ω is the angular velocity of the tool, and k is the kth cutting edge.

Before NUCT calculation, it should be judged whether single-edge cutting occurs at the axial height of z. Equation (1) could be used when axial depth of cut cannot be neglected. Correspondingly, Eq. (3) could be used when axial depth of cut could be neglected. When single-edge cutting occurs, the point P_{ex} (x_{ex}, y_{ex}) is on the previous cutting edge trajectory of the same cutting edge, which could be expressed as

$$\begin{cases} x_{ex} = ft_{ex} + R\sin(\omega t_{ex} - \pi k) + r\sin(\omega t_{ex} + \theta + \alpha(z_{ex})) \\ y_{ex} = R\cos(\omega t_{ex} - \pi k) + r\cos(\omega t_{ex} + \theta + \alpha(z_{ex})) \end{cases} \tag{8}$$

where t_{ex} is the previous cutting time which satisfies Eq. (5).

When multiple-edge cutting occurs, point P_{ex} (x_{ex}, y_{ex}) may be on the previous cutting edge trajectories of another cutting edge (in the range of the intersection points) or the same cutting edge (out of the range of the intersection points), which could be seen in Fig. 3. So, the intersection points of the cutting edge trajectories in feed direction must be calculated firstly. The intersection points satisfy the following conditions:

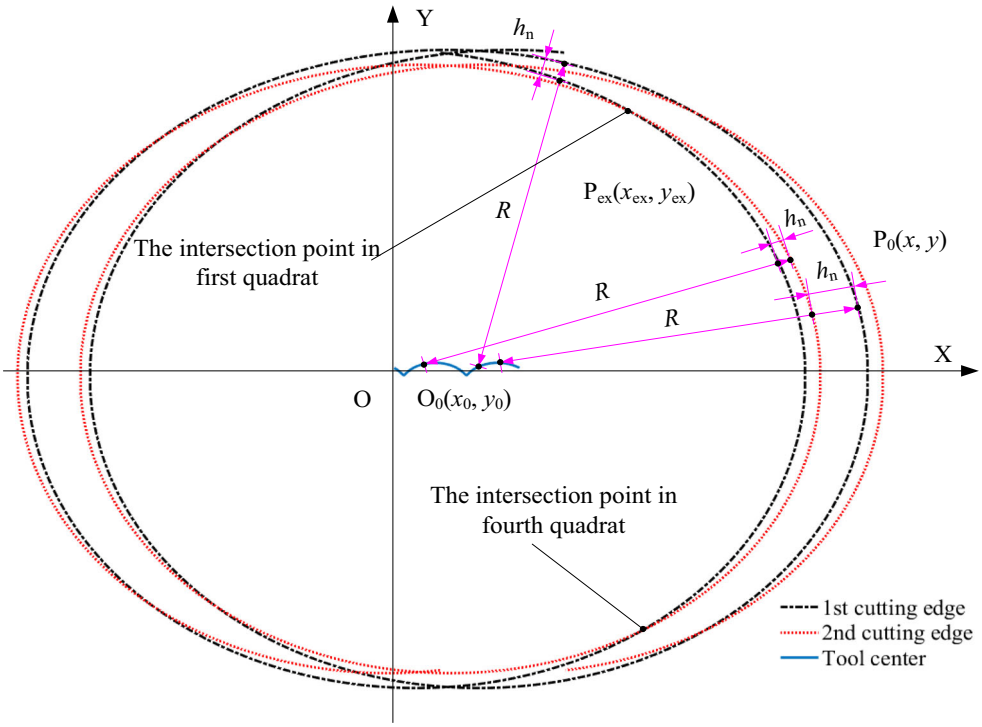

Fig. 3 Cutting edge trajectories at the axial height of z

$$\begin{cases} ft_1 + R\sin(\omega t_1 - \pi k_1) + r\sin(\omega t_1 + \theta + \alpha(z)) - ft_2 - R\sin(\omega t_2 - \pi k_2) - r\sin(\omega t_2 + \theta + \alpha(z)) = 0 \\ R\cos(\omega t_1 - \pi k_1) + r\cos(\omega t_1 + \theta + \alpha(z)) - R\cos(\omega t_2 - \pi k_2) - r\cos(\omega t_2 + \theta + \alpha(z)) = 0 \end{cases} \tag{9}$$

where t_1 and t_2 are the cutting times of k_1 and k_2 respectively. According to the characteristics of cutting edge trajectories, the initial values of t_1 and t_2 in the first quadrant are selected as 0 and π/ω respectively, and the initial values of t_1 and t_2 in the fourth quadrant are selected as π/ω and $2\pi/\omega$ respectively.

As shown in Fig. 3, NUCT of the second cutting edge is in the range of the intersection points and point P_{ex} (x_{ex}, y_{ex}) is on the previous cutting edge trajectory of the first cutting edge, which could be expressed as

$$\begin{cases} x_{ex} = ft_{ex} + R\sin(\omega t_{ex} - \pi(k-1)) + r\sin(\omega t_{ex} + \theta + \alpha(z_{ex})) \\ y_{ex} = R\cos(\omega t_{ex} - \pi(k-1)) + r\cos(\omega t_{ex} + \theta + \alpha(z_{ex})) \end{cases} \tag{10}$$

For the first cutting edge, when NUCT is in the range of the intersection points, point P_{ex} (x_{ex}, y_{ex}) is on the previous cutting edge trajectory of the second cutting edge which could be expressed by Eq. (10). When NUCT of the first cutting edge is out of the range of the intersection points, the first cutting edge is still single-edge cutting, point P_{ex} (x_{ex}, y_{ex}) is on the previous cutting edge trajectory of the same cutting edge, which could be expressed by Eq. (8).

Substituted Eq. (6), (7), (8), and (10) into Eq. (5), the following equation can be obtained:

when single-edge cutting occurs,

$$\begin{aligned} &\tan(\omega t - \pi k)(R\cos(\omega t - \pi k) + r\cos(\omega t + \theta + \alpha(z)) - R\cos(\omega t_{ex} - \pi k) - r\cos(\omega t_{ex} + \theta + \alpha(z_{ex}))) \\ &- ft - R\sin(\omega t - \pi k) - r\sin(\omega t + \gamma_0 + \alpha(z)) + ft_{ex} + R\sin(\omega t_{ex} - \pi k) + r\sin(\omega t_{ex} + \theta + \alpha(z_{ex})) = 0 \end{aligned} \tag{11}$$

when multiple-edge cutting occurs,

$$\begin{aligned} &\tan(\omega t - \pi k)(R\cos(\omega t - \pi k) + r\cos(\omega t + \theta + \alpha(z)) - R\cos(\omega t_{ex} - \pi(k-1)) - r\cos(\omega t_{ex} + \theta + \alpha(z_{ex}))) \\ &- ft - R\sin(\omega t - \pi k) - r\sin(\omega t + \theta + \alpha(z)) + ft_{ex} + R\sin(\omega t_{ex} - \pi(k-1)) + r\sin(\omega t_{ex} + \theta + \alpha(z_{ex})) = 0 \end{aligned} \tag{12}$$

Since axial component of the feed in the adjacent cutting period has little effect on the calculation of NUCT, it is assumed that z_{ex} is equal to z to simplify Eq. (11) and (12). Then, the unique unknown t_{ex} in Eq. (11) and (12) can be solved by iterative algorithm. The equations have complex structures and a huge amount of data, so the calculation time will be greatly extended if the initial value is not selected properly.

When single-edge cutting occurs, the initial value t_0 should be selected as

$$t_0 = t - 2\pi/\omega \tag{13}$$

when multiple-edge cutting occurs, t_0 should be selected as

$$t_0 = t - \pi/\omega \tag{14}$$

After the unknown t_{ex} is solved, coordinate values of the points O_0, P_{ex}, and P_0 could be obtained by Eq. (6), (7), (8), and (10), NUCT h_n (t, k, z) of the kth cutting edge at cutting time of t and axial height of z could be obtained by:

$$h_n(t,k,z) = R - \left((x_0 - x_{ex})^2 + (y_0 - y_{ex})^2\right)^{0.5} \tag{15}$$

3.2 Actual uncut chip thickness

Micro-milling has significant scale effects [16, 17]. When IUCT is less than the minimum chip thickness h_{min}, workpiece is elastically deformed and does not form chips; when IUCT is greater than or equal to the minimum chip thickness h_{min}, cutting chip will form, as shown in Fig. 4. The elastic recovery of the workpiece should be taken into account when calculating the actual uncut chip thickness (AUCT).

Thus, taking into account the scale effects, the AUCT h_a could be calculated as when single-edge cutting occurs,

$$\begin{cases} h_a(t,k,z) = h_a(t-2\pi/\omega,k,z) + h_n(t,k,z), \text{when } h_a(t-2\pi/\omega,k,z) < h_{min} \\ h_a(t,k,z) = h_n(t,k,z), \text{when } h_a(t-2\pi/\omega,k,z) \geq h_{min} \end{cases} \tag{16}$$

when multiple-edge cutting occurs,

$$\begin{cases} h_a(t,k,z) = h_a(t-\pi/\omega,k-1,z) + h_n(t,k,z), \text{when } h_a(t-\pi/\omega,k-1,z) < h_{min} \\ h_a(t,k,z) = h_n(t,k,z), \text{when } h_a(t-\pi/\omega,k-1,z) \geq h_{min} \end{cases} \tag{17}$$

Figure 5 shows cutting edge trajectories in single-edge cutting. It can be seen that if the cumulative elastic deformations of the first cutting edge is still less than the minimum chip thickness, another cutting edge may cut the elastic recovery part of the workpiece, but no material will be removed. Relative to single-edge cutting, this phenomenon could be called as "pseudo-single-edge cutting," which may only occurs when the NUCT is very small. The AUCT of pseudo-single-edge cutting has significance for predicting of cutting force, but it is difficult to be observed. In Fig. 5, when the AUCT of the first cutting edge elastic deform two times and the AUCT is still smaller than the minimum chip thickness, the second cutting edge will plowing cut the elastic recovery part of the workpiece. The cumulative cutting time m before forming the chip can be calculated by using the following formula:

$$m = \lceil h_{min}/2f_t \rceil \tag{18}$$

where the symbol "⌈ ⌉" is upper rounding function.

In single-edge cutting, the cutting edge which not involved in cutting is called "non-cutting edge" in this paper. The lag cutting cycle of the non-cutting edge (the second cutting edge in Fig. 5) n should be calculated as

$$n = \lceil -\zeta/2f_t \rceil \tag{19}$$

Pseudo-single-edge cutting occurs when m is greater than n. The AUCT of the non-cutting edge in pseudo-single-edge cutting is also based on the collinear points of O_0, P_{ex}*, and P_0, but the point P_{ex}* is on the nth previous cutting edge trajectory.

4 Results and discussions

4.1 NUCT in micro-end milling

The NUCTs and cutting parameters in micro-end milling are shown in Fig. 6. Figure 6 a shows the NUCTs when the tool

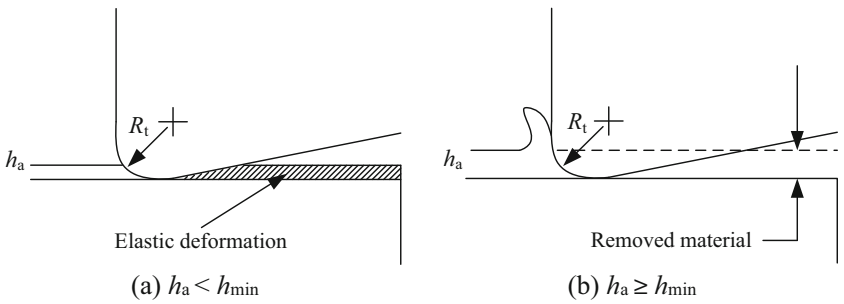

(a) $h_a < h_{min}$ (b) $h_a \geq h_{min}$

Fig. 4 Scale effect in micro-milling (R_t is tool edge radius). $h_a < h_{min}$ (**a**). $h_a \geq h_{min}$ (**b**)

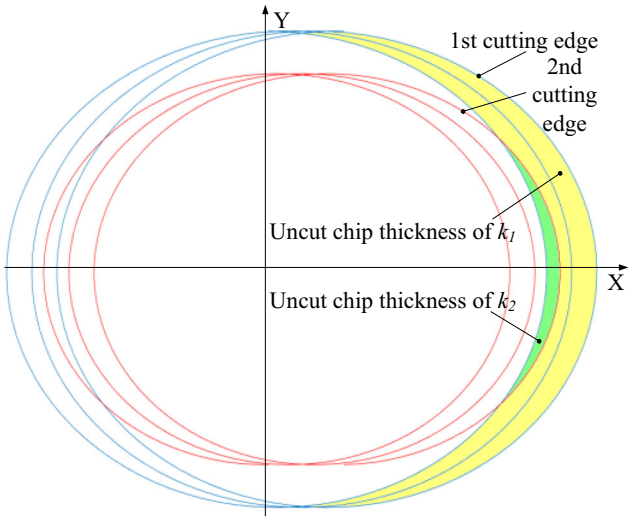

Fig. 5 AUCTs in single-edge cutting

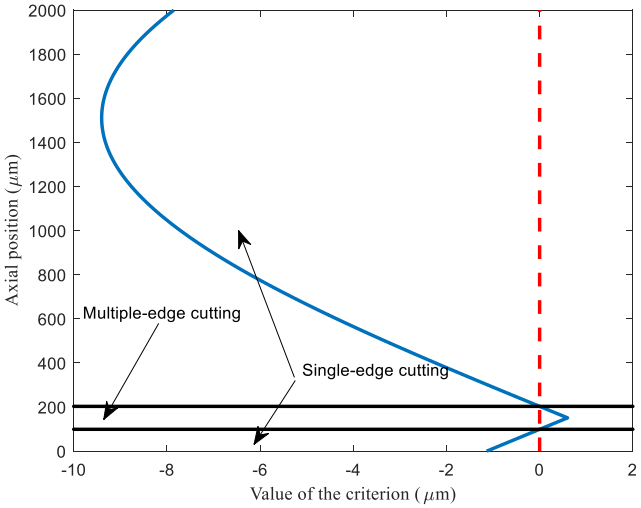

Fig. 7 The values of single-edge cutting criterion in effective cutting edge range ($R = 500$ μm, $r = 5$ μm, $\theta = 80°$, $f_t = 0.6$ μm)

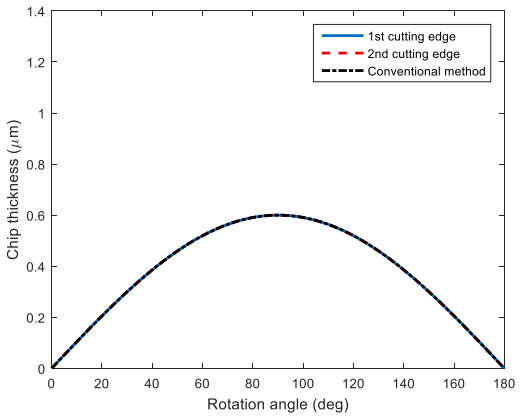

(a) When the tool has no runout (R=500 μm, r=0 μm, θ=0°, z=0 μm, f_t=0.6 μm, Ω=20000 rpm)

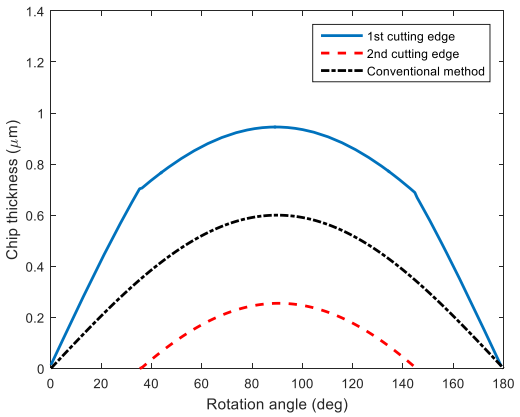

(b) When the tool has runout and multiple-edge cutting occurs (R=500 μm, r=5 μm, θ=88°, z=0 μm, f_t=0.6 μm, Ω=20000 rpm)

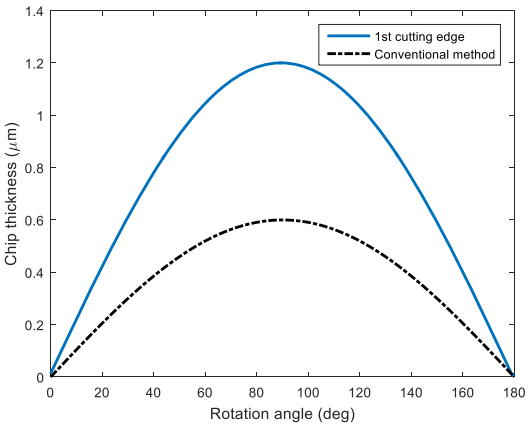

(c) When single-edge cutting occurs (R=500 μm, r=5 μm, θ=80°, z=0 μm, f_t=0.6 μm, Ω=20000 rpm)

Fig. 6 NUCTs of different cutting edge. When the tool has no runout ($R = 500$ μm, $r = 0$ μm, $\theta = 0°$, $z = 0$ μm, $f_t = 0.6$ μm, $\Omega = 20{,}000$ rpm) (**a**). When the tool has runout and multiple-edge cutting occurs ($R = 500$ μm, $r = 5$ μm, $\theta = 88°$, $z = 0$ μm, $f_t = 0.6$ μm, $\Omega = 20{,}000$ rpm) (**b**). When single-edge cutting occurs ($R = 500$ μm, $r = 5$ μm, $\theta = 80°$, $z = 0$ μm, $f_t = 0.6$ μm, $\Omega = 20{,}000$ rpm) (**c**)

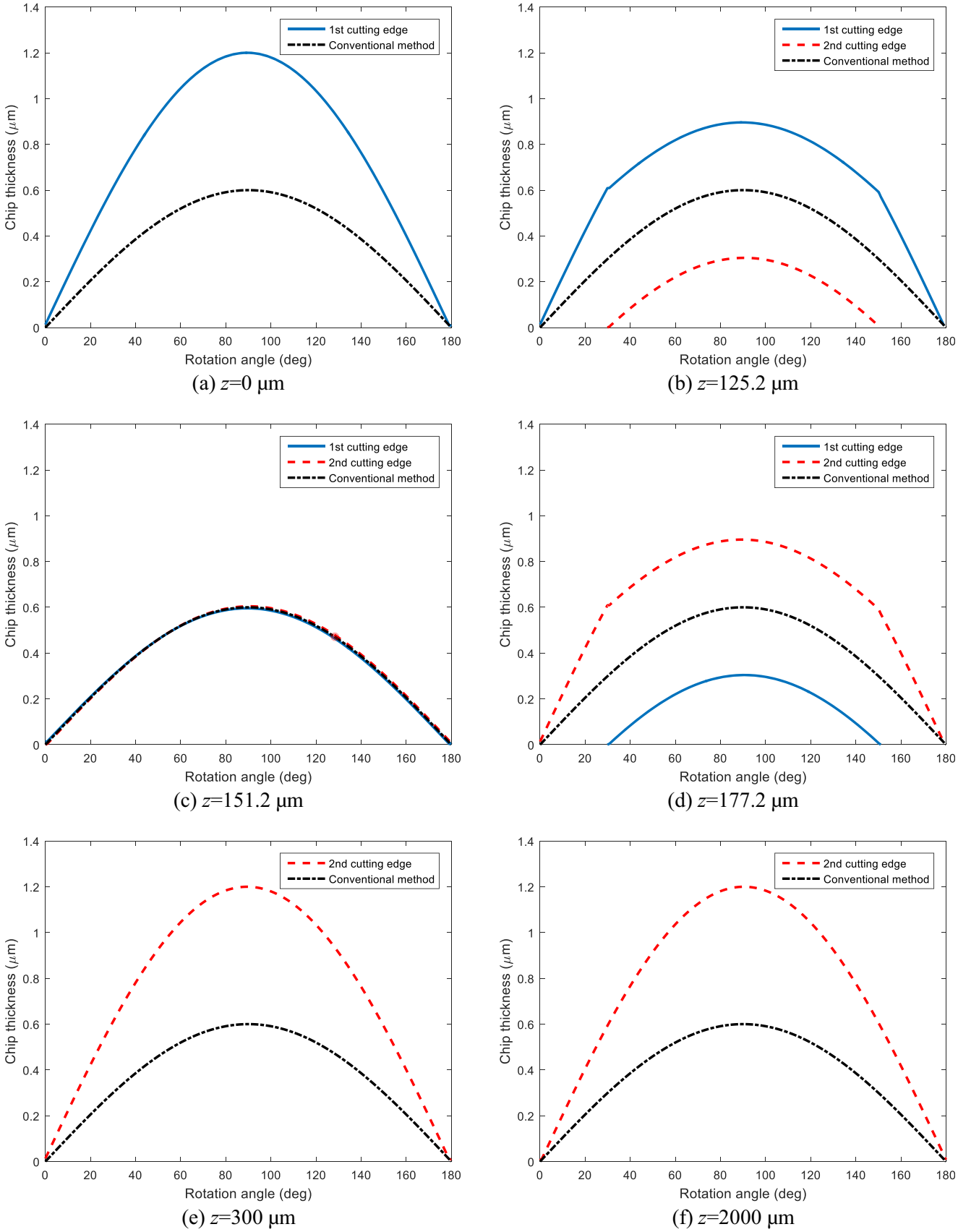

Fig. 8 NUCTs in different axial height $z = 0$ μm (**a**) $z = 125.2$ μm (**b**) $z = 151.2$ μm (**c**) $z = 177.2$ μm (**d**) $z = 300$ μm (**e**) $z = 2000$ μm (**f**) ($R = 500$ μm, $r = 5$ μm, $\theta = 80°$, $f_t = 0.6$ μm)

has no runout. The two cutting edges have the same NUCTs at the same position angle and the peak values of NUCTs are equal to feed per tooth. The IUCTs which are calculated by conventional method are also shown in the picture. The conventional method also shows good calculation accuracy when the tool has no runout. When the tool has runout and multiple-edge cutting occurs, the NUCTs are shown in Fig. 6 b. Under the influence of tool runout, NUCTs of the first cutting edge are much larger than that of the second cutting edge at the same position angle. The peak values of NUCTs of cutting edges are 0.945 and 0.255 μm respectively, and the sum of them is twice of the feed per tooth. The result of the IUCTs which calculated by the conventional method deviated greatly. When single-edge cutting occurs, only one cutting edge has the real NUCT. The peak value of NUCT is 1.2 μm, which is twice of the feed per tooth as shown in Fig. 6 c. The conventional method cannot be used to calculate the IUCT when single-edge cutting occurs.

4.2 NUCT in micro-side milling

According to Eq. (1), the distribution of single-edge cutting criterion value in the effective cutting edge range (0 to 2000 μm) can be obtained when tool radius, tool runout length, tool runout angle, and feed per tooth are 500 μm, 5 μm, 80°, and 0.6 μm respectively, as shown in Fig. 7.

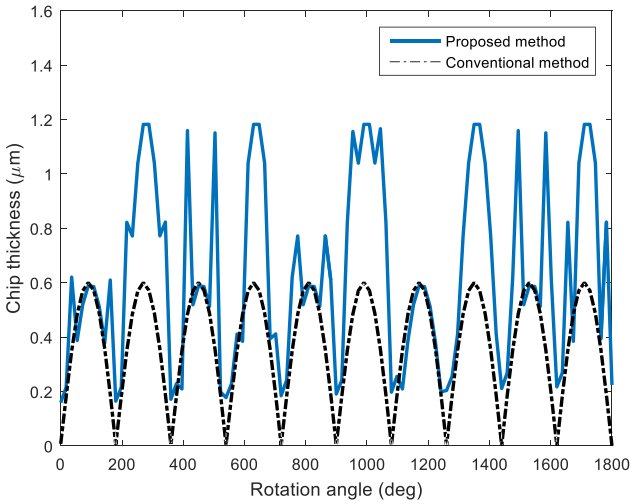

(a) When the tool has no runout
(R=500 μm, r=0 μm, θ=0°, f_t=0.6 μm)

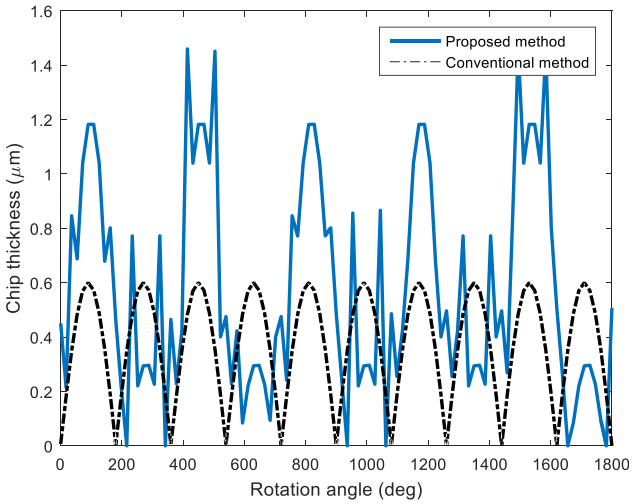

(b) When the tool has runout and multiple-edge cutting occurs
(R=500 μm, r=5 μm, θ=88°, f_t=0.6 μm)

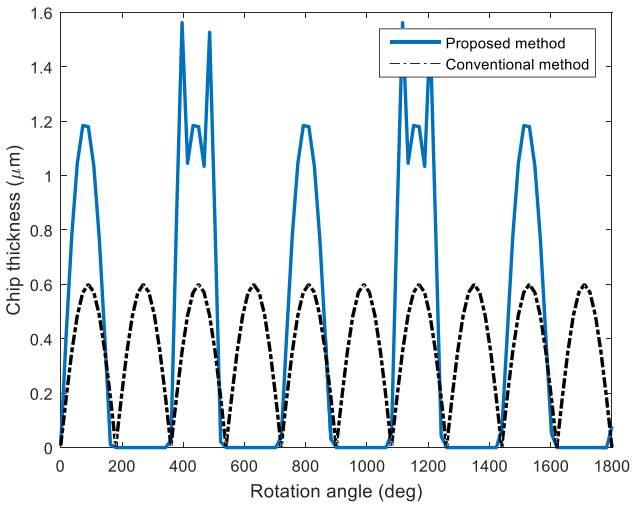

(c) When single-edge cutting occurs
(R=500 μm, r=5 μm, θ=80°, f_t=0.6 μm)

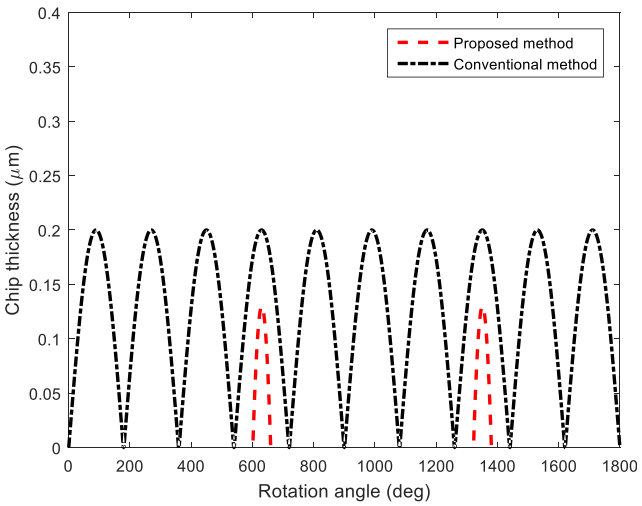

(d) When pseudo single-edge cutting occurs
(R=500 μm, r=5 μm, θ=85°, f_t=0.2 μm)

Fig. 9 AUCTs in different situations. When the tool has no runout (R = 500 μm, r = 0 μm, θ = 0°, f_t = 0.6 μm) (**a**). When the tool has runout and multiple-edge cutting occurs (R = 500 μm, r = 5 μm, θ = 88°, f_t = 0.6 μm) (**b**). When single-edge cutting occurs (R = 500 μm, r = 5 μm, θ = 80°, f_t = 0.6 μm) (**c**). When pseudo-single-edge cutting occurs (R = 500 μm, r = 5 μm, θ = 85°, f_t = 0.2 μm) (d)

From Fig. 7, it can be seen that multiple-edge cutting only occurs in the range of axial position from 99.2 to 203.2 μm (between the black lines) and the remaining positions are single-edge cutting.

According to the proposed NUCT algorithm described above, NUCTs at different axial heights were calculated. Single-edge cutting occurs in the range from 0 to 99.2 μm in the axial position. Only the first cutting edge has the real NUCTs, and the peak value of NUCT is twice of the feed per tooth, as shown in Fig. 8 a. In the range from 99.2 to 151.2 μm, single-edge cutting changing into multiple-edge cutting, NUCTs of the first cutting edge gradually decrease when NUCTs of the second cutting edge synchronously increase. Figure 8 b shows the NUCTs at the middle point of this axial position range. At the position of 151.2 μm in the axial position, NUCTs of the two cutting edges are substantially equal, as shown in Fig. 8 c. Single-edge cutting changing into multiple-edge cutting gradually, where the axial position is in the range from 151.2 to 203.2 μm. NUCTs of the first cutting edge decrease when NUCTs of the second cutting edge synchronously increase. Fig. 8 d shows the NUCTs at the midpoint of this axial position range. When the axial position exceeds 203.2 μm, single-edge cutting reappears and the second cutting edge becomes the real cutting edge. NUCTs in 300 and 2000 μm are shown in Fig. 8 e, f respectively.

4.3 AUCT results

According to the proposed method, the AUCTs in 5 rotation cycles are shown in Fig. 9, in which the minimum chip thickness is chosen as 0.8 μm [12]. Figure 9 a shows the AUCTs when the tool has no runout. Because of the size effects in micro-milling, AUCTs of the two cutting edges are different in each cutting cycle and the chip will form in each rotation cycle. Figure 9 b shows the AUCTs when the tool has runout and multiple-edge cutting occurs. AUCTs of the two cutting edges are greatly different in each cutting cycle and the chip will also form in each rotation cycle. Figure 9 c shows the AUCTs when single-edge cutting occurs. Under this condition, only one cutting edge has the real AUCT when the other cutting edge does not participate in cutting. However, the chip will also form in each rotation cycle. Figure 9 d shows the AUCTs of the non-cutting edge in single-edge cutting. Under the given cutting parameters, the non-cutting edge will cut the elastic recovery workpiece for every two rotation cycles. As shown in Fig. 9, size effect which includes intermittent chip formation and single-edge cutting has large effect on the AUCTs in micro-milling.

5 Conclusions

Due to the calculation, accuracy of IUCT is very important to model milling processes, a new method for determining the IUCT in micro-milling is proposed in this paper. Based on the work performed, the following conclusions can be drawn:

1. The effects of tool runout and single-edge cutting on NUCT have been analyzed. The results show that NUCTs are different when the tool has no runout, the tool has runout and multiple-edge cutting occurs, and single-edge cutting occurs. The conventional method cannot be used in micro-milling.
2. A new method for calculating NUCT in micro-milling has been proposed. The method takes into account the effects of single-edge cutting, tool runout, and helix lag angle, which can be used not only for micro-end milling, but also for micro-side milling.
3. The calculation method of AUCT in micro-milling has been proposed in which the intermittent chip formation and minimum chip thickness are considered. Furthermore, in some especial cutting parameters, pseudo-single-edge cutting may occur in single-edge cutting.
4. NUCTs in micro-end milling and micro-side milling are analyzed respectively. The results show that NUCTs of different cutting edges are not equal at the same axial depth of cut. However, NUCTs of the same cutting edge change with the axial positions of the tool because the tool runout angle changes along with the helix angle.
5. AUCTs are analyzed when the tool has no runout, the tool has runout and multiple-edge cutting occurs, and single-edge cutting occurs. The results show that the proposed method takes into account the scale effect of micro-milling and shows more details which is accurate and versatile. It provides a new approach for the needs of both analytical and numerical modeling of micro-milling process.

Funding This work is supported by the National Natural Science Foundation of China (NSFC, No.51605118) and the Fundamental Research Funds for the Central Universities (Grant No. HIT.NSRIF. 2016042).

References

1. Liu Y, Li PF, Liu K, Zhang YM (2017) Micro milling of copper thin wall structure. Int J Adv Manuf Technol 90(1–4):405–412
2. Yang SC, Liu WW, Zhang YH, Wan Q (2017) Experimental evaluation on micro-texture parameters of carbide ball-nosed end mill in

machining of titanium alloy. Int J Adv Manuf Technol 96(5–8): 1579–1589
3. Li HZ, Liu K, Li XP (2001) A new method for determining the undeformed chip thickness in milling. J Mater Process Technol 113(1–3):378–384
4. Zhang X, Pan XD, Wang GL (2018) Tool runout and single-edge cutting in micro-milling. Int J Adv Manuf Technol 96(1–4):821–832
5. Martellotti ME (1941) An analysis of the milling process. Trans ASME 63:677–700
6. Spiewak SA (1994) Analytical modeling of cutting point trajectories in milling. J Eng Ind Trans ASME 116(4):440–448
7. Spiewak SA (1995) An improved model of the chip thickness in milling. CIRP Ann-Manuf Technol 44(1):39–42
8. Montgomery D, Altintas Y (1991) Mechanism of cutting force and surface generation in dynamic milling. J Eng Ind Trans ASME 113(2):160–168
9. Altintas Y, Montgomery D, Budak E (1992) Dynamic peripheral milling of flexible structures. J Eng Ind Trans ASME 114(2):137–145
10. Bao WY, Tansel IN (2000) Modeling micro-end-milling operations. Part I: analytical cutting force model. Int J Mach Tools Manuf 40(15):2155–2173
11. Bao WY, Tansel IN (2000) Modeling micro-end-milling operations. Part II: tool run-out. Int J Mach Tools Manuf 40(15):2175–2192
12. Vogler MP, DeVor RE, Kapoor SG (2001) Microstructure-level force prediction model for micro-milling of multi-phase materials. J Manuf Sci Eng Trans ASME 125(2):202–209
13. Rodríguez P, Labarga JE (2015) Tool deflection model for micromilling processes. Int J Adv Manuf Technol 76(1–4):199–207
14. Jun MBG, Liu XY, DeVor RE, Kapoor SG (2006) Investigation of the dynamics of microend milling-part I: model development. J Manuf Sci Eng 128(4):893–900
15. Li CF, Lai XM, Li HT, Ni J (2007) Modeling of three-dimensional cutting forces in micro-end-milling. J Micromech Microeng 17(4): 671–678
16. Chae J, Park SS, Freiheit T (2006) Investigation of micro-cutting operations. Int J Mach Tools Manuf 46(3–4):313–332
17. Son SM, Lim HS, Ahn JH (2005) Effects of the friction coefficient on the minimum cutting thickness in micro cutting. Int J Mach Tools Manuf 45(4–5):529–535